Geomechanics and Engineering, *Vol. 25, No. 6 (2021) 439-454*
DOI: https://doi.org/10.12989/gae.2021.25.6.439

Influence of different combinations of measurement while drilling parameters by artificial neural network on estimation of tunnel support patterns

Jiankang Liu[1], Yujing Jiang*[2], Yuanchao Zhang[2] and Osamu Sakaguchi[3]

[1]*College of Energy and Mining Engineering, Shandong University of Science and Technology, Qingdao 266590, China*
[2]*Graduate School of Engineering, Nagasaki University, 1-14 Bunkyo-machi, 852-8521 Nagasaki, Japan*
[3]*Department of Civil Engineering, Konoike Construction Co., Ltd., 3-6-1, Kitakyuhoji-machi, Chuo-ku, 541-0057 Osaka, Japan*

(Received February 1, 2020, Revised July 3, 2020, Accepted June 8, 2021)

Abstract. In tunnel engineering, the selection of tunnel support patterns should be estimated accurately to ensure stability of the tunnel, which may be caused by unexpected hazardous zones ahead of tunnel face. This study presents a method to estimate the selection of support patterns using artificial neural network (ANN) based on 318, 649 Measurement While Drilling (MWD) data. Controlled trials are conducted considering different input layer sizes and hidden layer sizes to obtain the optimal ANN model. Combinations of 6 feature parameters including penetration rate (PR), hammer pressure (HP), rotation pressure (RP), feed pressure (FP), hammer frequency (HF) and specific energy (SE) correspond to the different input layer sizes of the ANN. Average accuracy (A), average computing-time (T), sensitivity and stability are adopted as the performance index. The results show that a strong correlation exists between MWD data and support patterns. The combination of 6 feature parameters outperforms the subset of the entire feature parameters in terms of A, sensitivity and stability. The ANN model with the combination of PR, HP, RP, FP, HF and SE as the input feature parameters has the highest estimation stability. The ANN model with 6 feature parameters and one hidden layer with 30 nodes is proposed as optimal model considering all indices. The results confirm that it is feasible to estimate support patterns ahead of tunnel face using ANN based on MWD data.

Keywords: tunnel support pattern; feature selection; measurement while drilling data; artificial neural network

1. Introduction

As a mountainous country, in most cases, mountain tunnels are indispensable for transportation such as railways and highways in Japan. The stability of such tunnels is generally affected by hazardous geological conditions such as cavities or water bearing, fractured, or relatively stronger zones (Miura 2003, Gong *et al.* 2013, Mikaeil *et al.* 2016, Liu *et al.* 2020, Zhou *et al.* 2020). In the mountain tunnel design process, engineers perform a geotechnical investigation generally by means of surface exploration e.g., borehole drilling, geophysical exploration, and geologic mapping, to yield estimates of overall geological profiles (Dahlin *et al.* 1999, Soupios *et al.* 2008, Kun and Onargan 2013, Park *et al.* 2017). Unexpected geological conditions may occur if only depending on the crude drawings of overall geological profiles, which seriously threaten the tunnel support stability (Kontogianni *et al.* 2004, Li *et al.* 2012, Wang and Meng 2018). During the excavation, advanced Measure While Drilling (MWD) technology (Schunnesson 1997) implemented in construction site can provide more accurate geological condition information ahead of tunnel face (Friant *et al.* 1997, Lindén 2005, Nilsen 2015, Navarro *et al.* 2018, van Eldert *et al.* 2019). Furthermore, numerous successful applications of artificial neural network (ANN) technology in engineering cases make it possible to estimate the selection of support patterns ahead of tunnel face (Yang and Zhang 1997, Rafiq *et al.* 2001, Guan *et al.* 2009, Zhang *et al.* 2017, Ghorbani *et al.* 2018, Kwon and Lee 2018, Koopialipoor *et al.* 2019).

It is necessary to grasp precisely the geological conditions ahead of tunnel face to ensure the effectiveness of the selected tunnel support pattern (Singh *et al.* 1992, El-Naqa 2001, Bizjak and Petkovšek 2004, Kaya *et al.* 2011, Elyasi *et al.* 2016). In geological engineering, many researchers have carried out the study of evaluating geological conditions by MWD method. Schunnesson (1998) has focused on MWD extensively and analyzed the correlation between the MWD data and the characteristics of specific rock class. The potential of for RQD (Rock Quality Designation) classification ahead of the tunnel face from MWD data was pointed out. Segui and Higgins (2002) concluded that with the elimination of human errors in classification and the development of automated logging systems, MWD data can provide an accurate description of the rock mass. Ghosh *et al.* (2015) evaluated data trends among logged parameters and calculated average specific energy (SE) by MWD data. It demonstrated that there is a significant hole length dependency for penetration rate (PR) and feed pressure (FP) affecting the predicted specific energy. Galende-Hernández *et al.* (2018) introduced an MWD based methodology for support tunnel construction: Rock Mass Rating (RMR) estimation was provided by excavation surface features and expert knowledge based on MWD data. The results showed a good and serviceable

*Corresponding author, Professor
E-mail: jiang@nagasaki-u.ac.jp

ISSN: 2005-307X (Print), 2092-6219 (Online)

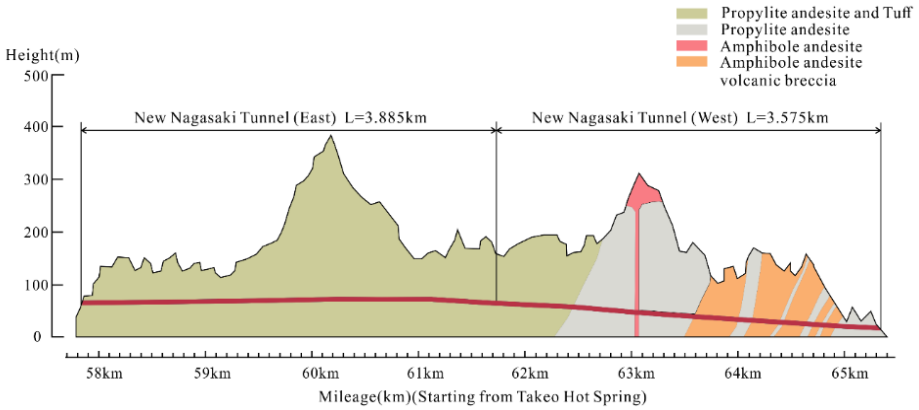

Fig. 1 Long section of the new Nagasaki tunnel

Table 1 Description details for the six support patterns

Class No.	Support patterns	Number of bolts	Space of bolts (mm)	Class of I-beam	Shape of I-beam	Eccentric or not	Initial lining thickness (cm)	Secondary lining thickness (cm)
Class 1	II-A(B)	10	1500	H100		N	10	30
Class 2	I-2-A(B)	10	1200	H125		N	12.5	30
Class 3	I-2-B(B)	10	1200	H125		Y	12.5	30
Class 4	II-B(B)	10	1500	H100		Y	10	30
Class 5	I-2-B(B)C	6	1200	H125		Y	12.5	30
Class 6	I-2-B(B)D I-2-B(B)E	6	1200	H125		Y	12.5	30

performance. The above researches confirm that the MWD data can characterize the geological condition of rocks. However, the possibility of using such measured data directly to estimate the support patterns ahead of tunnel face requires further investigate.

Artificial neural network (ANN) is one artificial intelligence (AI) application which imitates the structure and behavior of neurons in the human brain and can be trained to recognize and categorize complex patterns (Ben Ali *et al.* 2015, Xue 2019). Pattern recognition is carried out by training and adjusting the parameters of the ANN through error minimization process (Lo *et al.* 1995, Basu *et al.* 2010). They can be calibrated using any class of input data, such as MWD data and corresponding rock quality designation (RQD) and the output can be classified into any given number of categories (Kumar *et al.* 2019). ANN has been recently applied to tunnel engineering problems, such as classification of rock mass rating (Qiu *et al.* 2014, Nikafshan Rad *et al.* 2015, Hussain *et al.* 2016), prediction of tunnel convergence (Yi *et al.* 2006, Mahdevari and Torabi 2012, Mahdevari *et al.* 2012) and surface settlement (Kim *et al.* 2001, Suwansawat and Einstein 2006, Ocak and Seker 2013). For rock support, Utt (1999) pointed out that based on the ANN technology, the MWD data can be converted into the characteristics of appropriate proportion, and the strength of the formation can be classified. In 2002, the real-time monitoring system using ANN to estimate the strength of continuous strata was reported in detail by Utt *et al*. (2002), and the feasibility of the system was verified in the laboratory. Leu *et al.* (2001) proposed a data mining method for the prediction of tunnel support stability by ANN, and the results showed that ANN is superior to the traditional discriminant analysis and multiple nonlinear regression method in the prediction of tunnel support stability. Based on machine learning and computational intelligence technology, Galende-Hernández, Menéndez, Fuente and Sainz-Palmero (2018) used MWD data to estimate rock mass rating. The results indicated that the accuracy of this method is high, and the error is about 3%. However, the studies involving the estimation of support patterns ahead of tunnel face based on MWD data using ANN, have not been reported.

In this study, the ANN was used to estimate the support patterns ahead of the tunnel face based on the MWD data. A total of 318, 649 MWD data sets obtained along the whole length of a tunnel ware used for this assignment. Also, the feasibility of using ANN to estimate the support patterns based on the MWD data was investigated. The effects of different neural network structures on the estimation performance of the ANN for tunnel support patterns were analyzed. Furthermore, all possible combinations of the six MWD parameters were used to evaluate the estimation performance. The sensitivity of each feature to the estimation performance of the ANN was compared. The stability of the estimation performance of the superior ANN models were analyzed as well. Finally, the ANN model with optimal estimation performance was recommended.

2. Data collection

The new Nagasaki tunnel is the longest (7.46 km) tunnel of West Kyushu Line in Japan, which is divided into two working areas: east and west (Fig. 1). The tunnel is constructed by 3.885 km in the east and 3.575 km in the

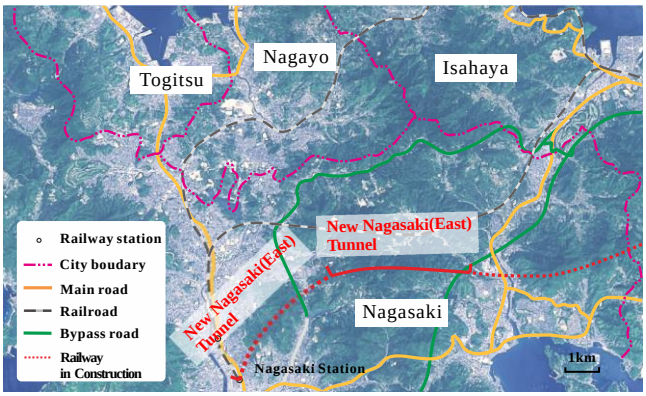

Fig. 2 Location of new Nagasaki (east) tunnel

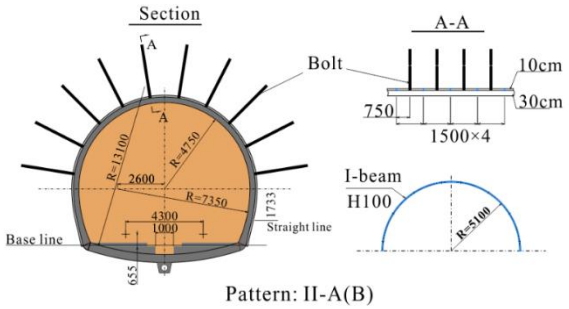

Fig. 3 Section diagram of support pattern of class 1

(a) The hydraulic percussion drill

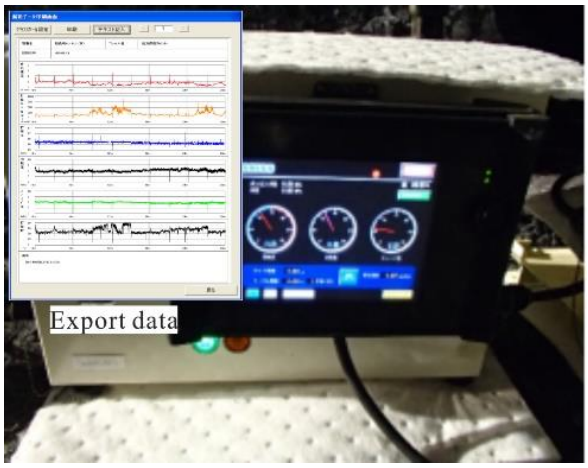

(b) The measure while drilling device

Fig. 4 The drill and data collection device

west as shown in Fig. 2. Among them, the new Nagasaki tunnel (east) was completed in 2017. In the present study, 318, 649 drilling data sets was obtained in the tunnel project from 97 drill holes. The tunnel was excavated by the method of New Austrian Tunneling Method. In this tunnel construction, many support patterns were applied, namely I-2-A(RC)(B), I-2-A(B), I-2-A(C), I-2-A(D), I-2-B(B), I-2-B (B) C, I-2- B(B) D [I-2-B (B) E], I-2- B (B) F, II-A-B(B) and II-B(B). It should be noted that except for part of the data [comprising the support patterns I-2-A(RC)(B), I-2-A(C), I-2-A(D) and I-2- B (B) F, totaling about 190 meters] cannot collected, the support patterns corresponding to the remaining data sets were divided into six classes according to number of bolts, space of bolts, Class and shape of I-beam, initial and secondary lining thickness and eccentric or not. The comparison of details of the six support patterns are listed in Table 1. Fig. 3 shows the section diagram of support pattern of class 1.

The MWD technology can provide accurate and objective description of rock mass characteristics and be used to design the final rock support. The recorded MWD data is the response of different rock mass characteristics. It has proved to be an objective and reliable method to evaluate the rock mass conditions ahead of a tunnel face (Schunnesson 1996, Schunnesson *et al.* 2011, Humstad *et al.* 2012, van Eldert *et al.* 2017). Fig. 4(a) shows a

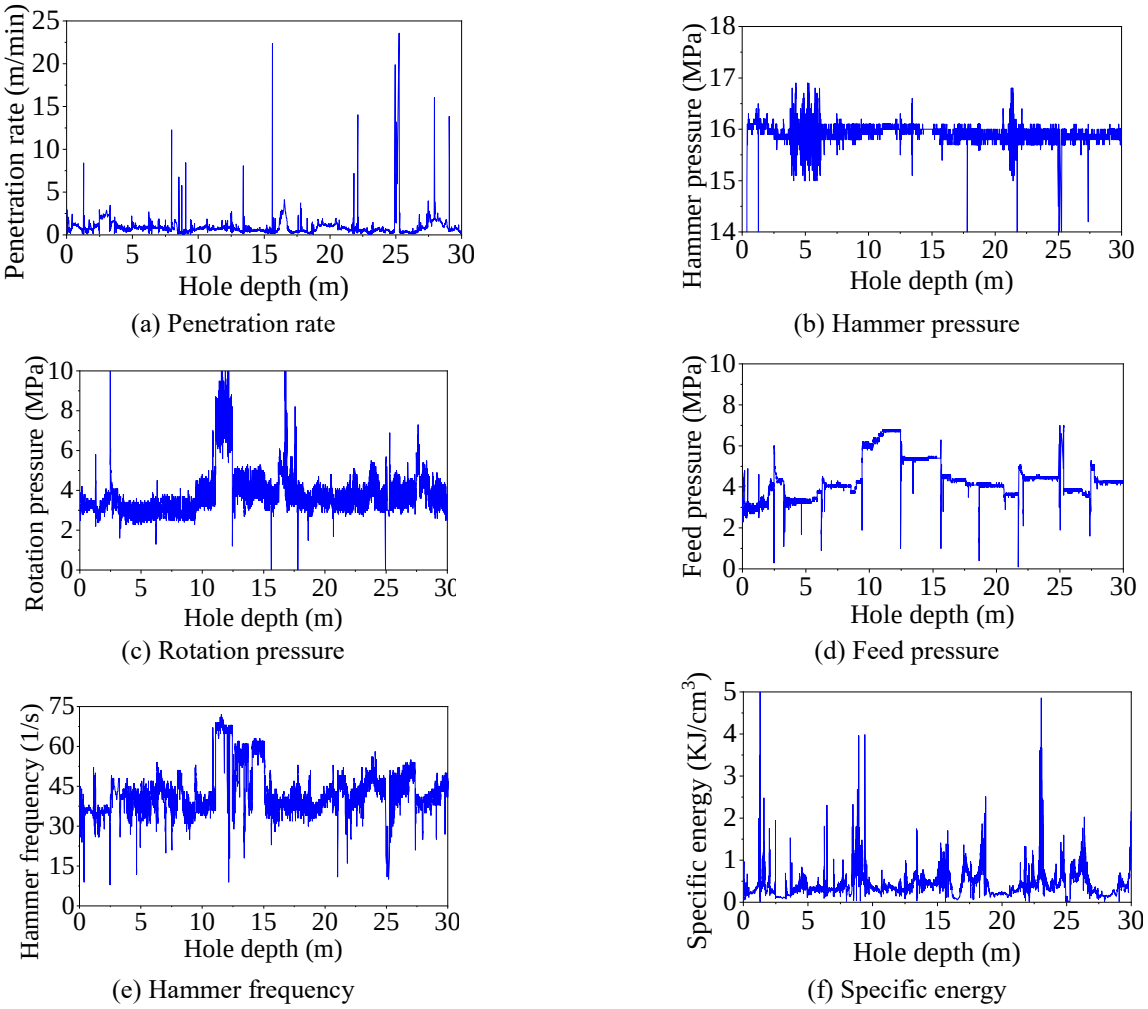

(a) Penetration rate (b) Hammer pressure

(c) Rotation pressure (d) Feed pressure

(e) Hammer frequency (f) Specific energy

Fig. 5 Visualization of drilling data collected from one bolt borehole

photograph of hydraulic percussion drill used in this study for drilling investigation ahead of tunnel face. This drilling equipment is equipped with drilling data logging system to measure and record the drilling data. The model of drilling rig is JTH3200R-III with the number of booms of 3. The he drilling mode is semi-automatic. The length of drill pipe is 3 m and the diameter of drill bit is 65 mm. The length of standard sampling borehole is 30-45 m. All MWD data are output from the data collection device in approximately every 0.25 seconds. The MWD data is collected and recorded by a data collection device (as shown in Fig. 4b) connected to the drilling equipment which can record the oil pressure data when drilling. The excavation of the tunnel needs to be stopped before the drilling procedure starts. The drilling procedure includes adjusting the position of the drilling equipment and the drill pipe, drilling, data recording, connecting the drill pipe, and withdrawing the drill pipe. The MWD data (as shown in Fig. 5) obtained from the data collection device include PR, Hammer pressure (HP), rotation pressure (RP), FP, hammer frequency (HF) and SE. The RP represents the speed of the drill pipe during drilling, which can be used to judge whether it is fragile or soft geology. The HP is the force transmitted from drill pipe to rock during drilling, which is sensitive to the hardness of rock. The RP is a kind of pressure applied to rotate the drill pipe. When the pressure increases, it can be judged that there are some geological changes such as the appearance of weak layer and clay layer. The FP is the hydraulic oil pressure applied when the drill pipe rotates and impacts, which is generally affected by the strength of the rock. The HF represents the frequency of the drill pipe hitting the rock, and the higher frequency generally means that the broken rock is harder. The SE is a composite parameter, which refers to the energy consumed to destroy the rock per unit volume, as shown in Eq. (1):

$$E_s = \frac{ALN_s f}{vS} \times k \tag{1}$$

where E_s is the SE (J/cm^3), f is HF (1/min), v is PR (cm/min), S is cross-sectional area of the drill hole (cm^2), k is loss coefficient, A is piston com pression area (cm^2), L is piston stroke(cm), N_s is the hammer pressure (MPa or N/mm^2).

In the process of drilling, the working environment must be close to the ideal state. However, because the parameters obtained by the drilling system are not stable, there are many influencing factors, such as: the conditions with bit shape, flushing fluid, slag discharge state, bit diameter, etc., as well as the technical level difference of the drilling operator. In the actual drilling process, the ideal state does

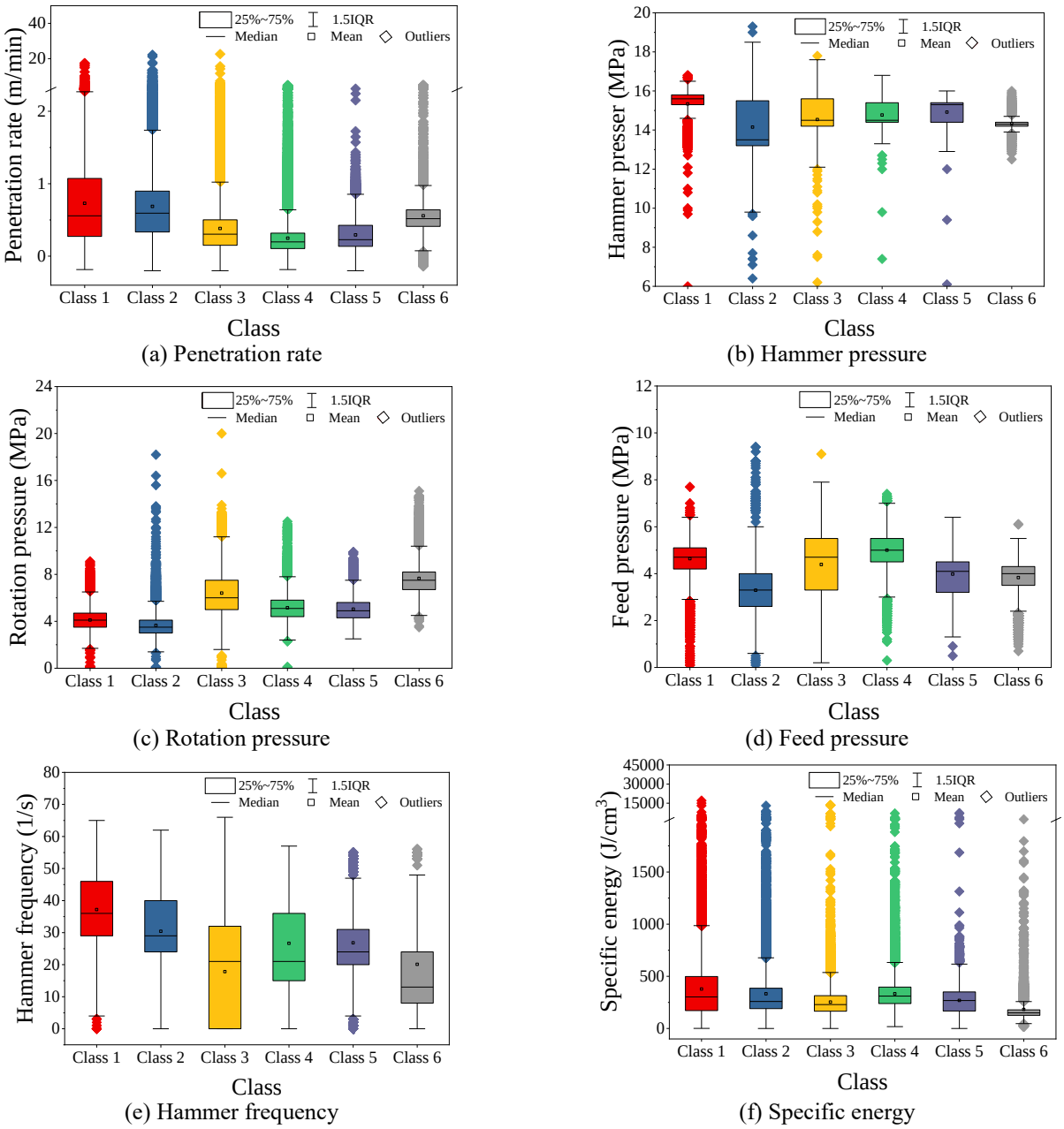

Fig. 6 Distribution of feature parameters of the input data

Table 2 Basic descriptive statistics for the original measure while drilling data of all drill holes

	Support pattern	Number of datasets	Number of bolts	Penetration rate (m/min)	Hammer pressure (MPa)	Rotation pressure (MPa)	Feed pressure (MPa)	Hammer frequency (1/s)	Specific energy (J/cm^3)
			Ave.	0.93	15.33	4.10	4.64	37.19	378.32
Class 1	II-A(B)	66514	Min.	0.02	6.00	0.00	0.10	0.00	1.00
			Max.	17.44	16.80	9.10	7.70	65.00	17028.00
			Ave.	0.89	14.15	3.65	3.29	30.43	332.69
Class 2	I-2-A(B)	49228	Min.	0.00	5.10	0.00	0.10	0.00	0.00
			Max.	22.16	19.30	18.20	9.40	62.00	13062.80
			Ave.	0.58	14.54	6.40	4.39	17.82	253.51
Class 3	I-2-B(B)	75767	Min.	0.00	5.6	0.00	0.20	0.00	0.00
			Max.	22.58	17.8	20	9.1	66	13598

Table 2 Continued

	Support pattern	Number of datasets	Number of bolts	Penetration rate (m/min)	Hammer pressure (MPa)	Rotation pressure (MPa)	Feed pressure (MPa)	Hammer frequency (1/s)	Specific energy (J/cm^3)
			Ave.	0.45	14.77	5.15	5.00	26.66	332.11
Class 4	II-B(B)	81976	Min.	0.02	5.20	0.00	0.30	0.00	18.30
			Max.	4.99	16.80	12.5	7.40	57.00	7013.40
			Ave.	0.49	14.92	5.03	3.98	26.84	269.11
Class 5	I-2-B(B)C	35413	Min.	0.00	6.10	2.50	0.50	0.00	0.00
			Max.	3.01	16.00	9.90	6.40	55.00	7210.80
			Ave.	0.76	14.33	7.65	3.83	20.10	182.98
Class 6	I-2-B(B)D	9751	Min.	0.06	12.50	3.50	0.70	0.00	16.90
			Max.	4.99	16.00	15.10	6.10	56.00	2389.50

not exist, so the response between the MWD parameters obtained by the drilling equipment and the physical properties of the rock is not high from the visual point of view. Therefore, this paper aims to use a powerful ANN technology to analyze the relationship between these data and the physical properties of the rock.

In the first stage of the study, an ANN for estimating the class of tunnel support patterns was constructed by using the recorded MWD data. The MWD data parameters (PR, HP, RP, FP, HF and SE) have been used as input feature parameters and the class numbers have been used as output parameters. The statistics of the maximum, minimum and average value of each parameter of different classes are presented in Table 2. As can be seen in Table 2, there is a difference in the average value of the MWD parameters related to each Class. It should be noted that a small number of singular values exist in the MWD data in Table 2, which is due to the original data collected by the project. In order to investigate the robustness of ANN, the original data are not filtered in this paper. This is also for the development of real-time prediction system based on ANN technology as a preliminary study. In order to reduce the influence of the order of magnitude difference among the feature parameters on the prediction performance of ANN, the input data was normalized to the range of 0-1 by the following Eq. 2. This normalization process is a common practice before the establishment of ANN model.

$$X_{norm} = \frac{x - x_{min}}{x_{max} - x_{min}} \quad (2)$$

where X_{norm} and x are normalized and measured data, respectively. x_{min} and x_{max} are the minimum and maximum value, respectively, of x.

Additionally, Fig. 6 compares the distribution of feature parameters. It can also be seen from the figure that the average values of the MWD parameters are different for each Class. However, it is indispensable to further study the correlation of the six feature parameters and whether there is information redundancy in the case when all six feature parameters are used as input data of the neural network. In the remaining subsections, neural network structure optimization and the input feature selection problem will be analyzed.

3. Methods

3.1 ANN

ANN is an information processing pattern developed by McCulloch and Pitts (1943) by simulating human brain. It consists of three layers: input layer, hidden layer and output layer. Each layer consists of nodes, which are sets of interconnected processor elements. The output of each layer is used as the input of the next layer. The output of any layer could be connected to the next layer using weighting factors based on their strengths or weaknesses. Moreover, linear or sigmoid colon functions are used as activation functions to calculate the output of neurons in each layer (Hsu *et al.* 1995).

For input and output layer, it should be noted that the number of nodes is determined by the number of variables in these layers. For the hidden layer, many researches (Hecht-Nielsen 1987, Hush 1989, Ripley 1993, Paola 1994, Kanellopoulos and Wilkinson 1997) have proposed heuristic methods to determine the number of nodes. However, there is no definite standard. To train ANNs, the most commonly adapted algorithm is error back-propagation algorithm (Dreyfus 2005, Toghroli *et al.* 2014). For minimizing the model error between goal standards and output, back-propagation algorithm is extremely suitable. Whenever the error of model is greater than predefined error, the network weights are adjusted by the system through back propagation. Consequently, in this study, the error back-propagation algorithm was employed for training. Fig. 7 shows the outlook of structure of the error back-propagation neural network (BPNN) model. Fig. 7 shows that each input node of BPNN model represents each MWD parameter, and the output nodes represent six support models. The main flow of BPNN algorithm includes: Step 1 initialize network, Step 2 calculate outputs of hidden layer, Step 3 calculate outputs of output layer, Step 4 calculate the error, Step 5 update weight and threshold, Step 6 judgment of iteration results. The details of the algorithm are illustrated in Fig. 8.

3.2 Parameter settings

In this study, MATLAB software has been used for

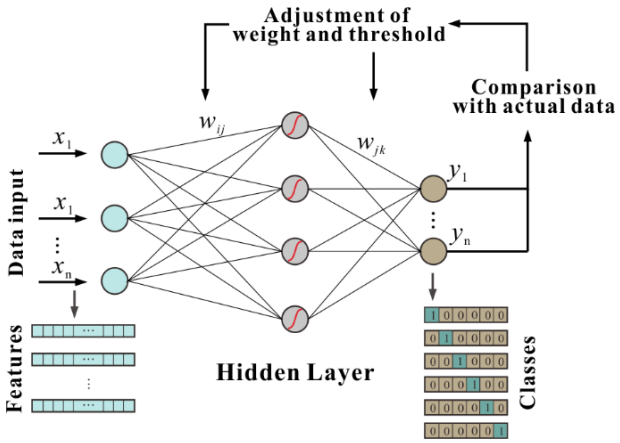

Fig. 7 Structure of error back-propagation neural network

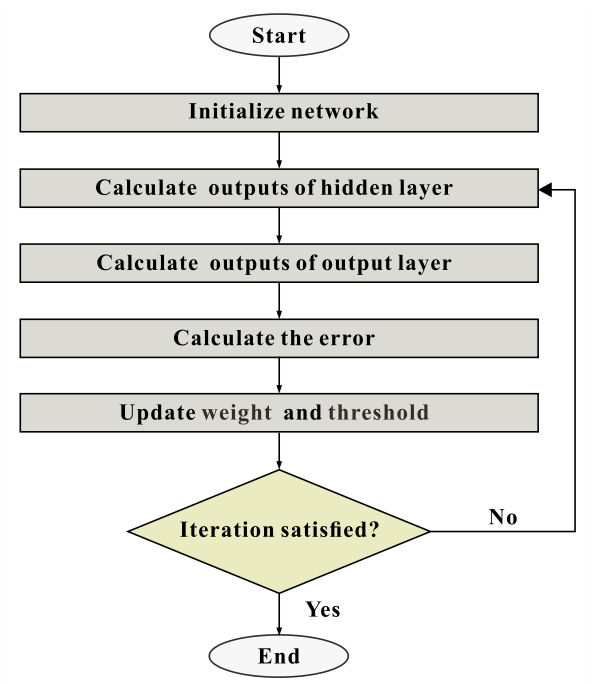

Fig. 8 Flow chart of artificial neural network algorithm

development of BPNN model. It should be noted that in order to automate the processing as much as possible this study develops the code of the BPNN model, without using built-in ANN tool of the software. For model training, if the selected learning rate value is larger, the modification of the weight will be greater and the network convergence will be faster. However, too small learning rate value will slow the convergence of the network and make the weight difficult to stabilize. The momentum term can be used to improve the convergence while reducing the oscillations of updating process of weights. In this study, after several trials, learning rate of 0.01 and momentum factor of 0.5 have been set to ensure the convergence of the algorithm. For the number of hidden layers, Kanellopoulos and Wilkinson (1997) stated that a second hidden layer is recommended when the output layer of the neural network has 20 (or more) nodes. Garson (1998) and García-Pedrajas *et al.* (2005) reported that a single hidden layer is usually sufficient to solve most problems, especially classification tasks. Thus, one hidden layer was preferred in this study. For the number of nodes in the input layer, it was equal to the number of feature parameters. Therefore, the input layer size can be calculated by multiplying the number of input layer nodes by the number of corresponding training sample data of each node. In order to evaluate the effect of different combinations of feature parameters as input data on the estimation performance of ANN models, different combinations of feature parameters and different number of hidden layer nodes were set up. In all cases, the number of nodes in output layer was equal to 6 corresponding to six tunnel support patterns. Sigmoidal activation function was used for modeling the transformation of values across the layers. In addition, randomly selected 6000 data sets (corresponding to 1000 data sets of each class of support patterns) from the total data sets were used in the training stage as training samples, and randomly selected 600 data sets (corresponding to 100 data sets of each class) were used in testing stage as testing samples.

4. Experimental results and discussion

4.1 Setting of the experiments

To ensure selection of the optimal combination of feature parameters, an analysis was performed with the data sets obtained from the tunnel construction site described in section 2. In this subsection, various experiment cases on 63 datasets were implemented. These cases aim to evaluate the performance of the BPNN with the different combinations of the feature parameters and the different number of hidden layer nodes. It must be pointed out that the marks P1, P2, …, P6 refer to the six feature parameters as shown in Table 3. In order to avoid the influence of different hardware specifications on the calculation time of the same code, all these cases were performed on the same PC with the same specification. The detailed specification parameters are presented in Table 4. Also, it must be highlighted that ID1-1, ID1-2, …, ID6 in Table 5 refer to the full combinations of the six feature parameters. In order to ensure the accuracy of the experiment, each experiment case was conducted 10 times under the same experimental conditions (the same combination of the feature parameters,

Table 3 The marks the six feature parameters

Feature parameters	Penetration rate	Hammer pressure	Rotation pressure	Feed pressure	Hammer frequency	Specific energy
Symbol	PR	HP	RP	FP	HF	SE
No.	P1	P2	P3	P4	P5	P6

Table 4 PC specification

	Penetration rate
CPU	Core (TM) i7
Frequency	4.00GHZ
RAM	20GB
Operating system	Windows 10

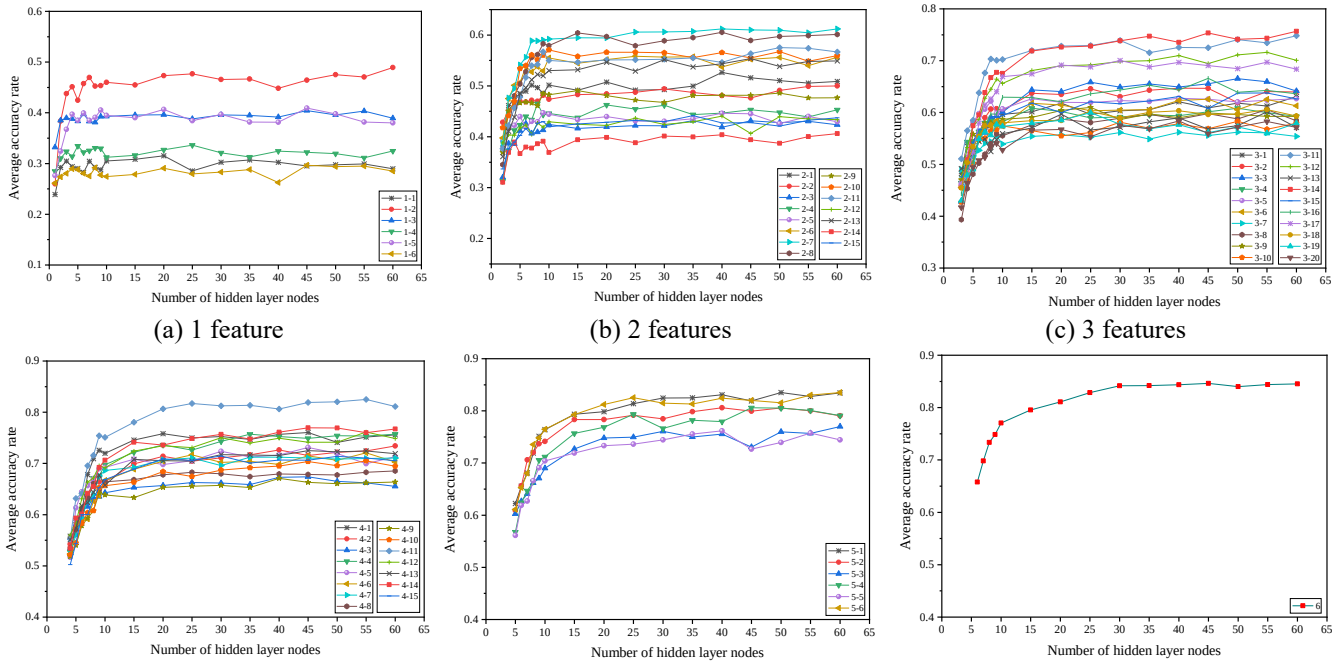

(a) 1 feature (b) 2 features (c) 3 features

(d) 4 features (e) 5 features (f) 6 features

Fig. 9 Variations of the average accuracies with the different number of hidden layer nodes and different number of the feature parameters

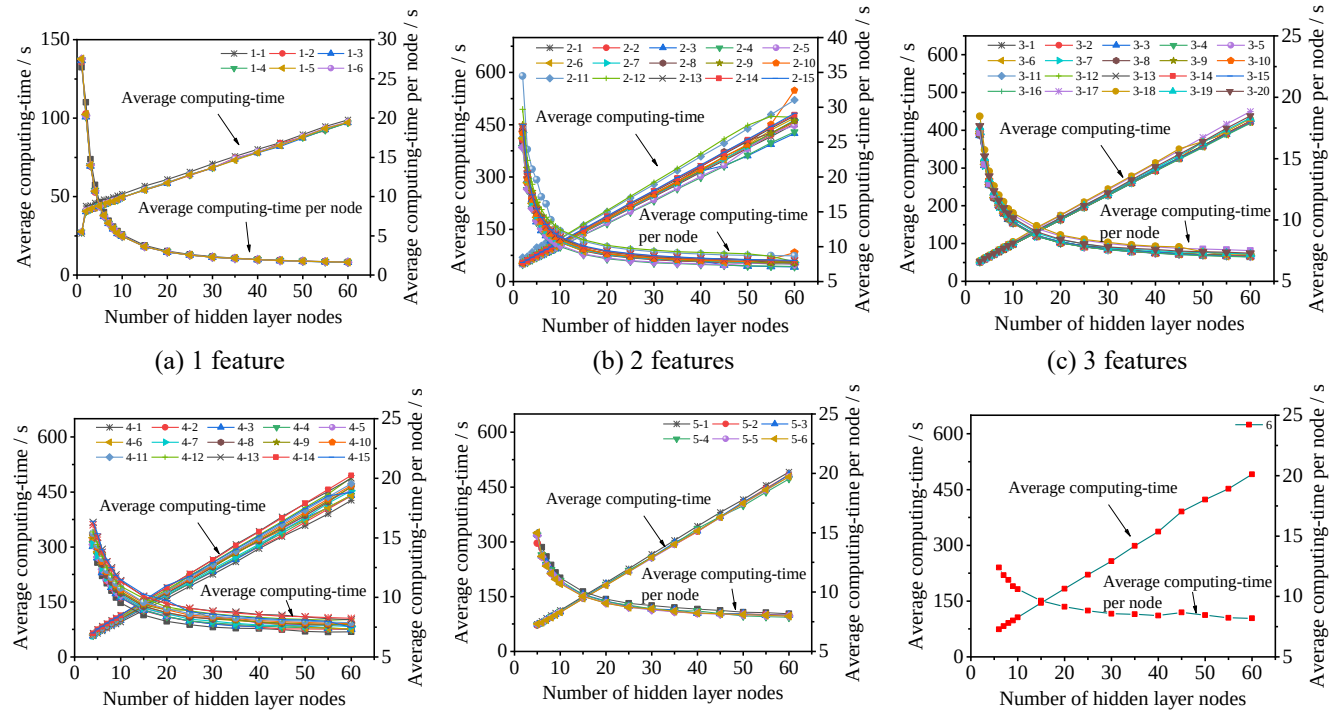

(a) 1 feature (b) 2 features (c) 3 features

(d) 4 features (e) 5 features (f) 6 features

Fig. 10 Variations of the average computing-times and the average computing-times per node with the different number of hidden layer nodes and the different number of the feature parameters

the same number of hidden layer nodes). Accuracy (A, A = the correctly predicted number of output samples / total number of output samples), computing-time (T), sensitivity and stability were taken as the performance indices. And, average accuracy ($\bar{A}$, $\bar{A}$ = A / 10) and average computing-time ($\bar{T}$, $\bar{T}$= T / 10) were obtained from 10 experiment cases under the same experimental conditions.

4.2 Performance of BPNN with different experimental conditions

A comparison between using whole feature length and

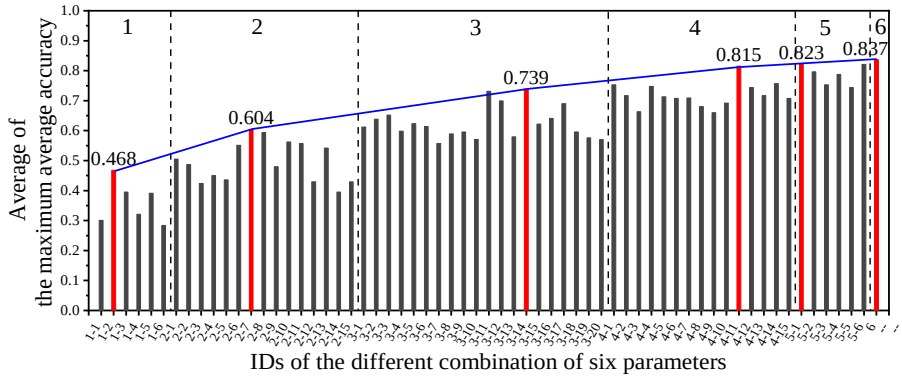

Fig. 11 The optimal average accuracies with the different combinations of six parameters

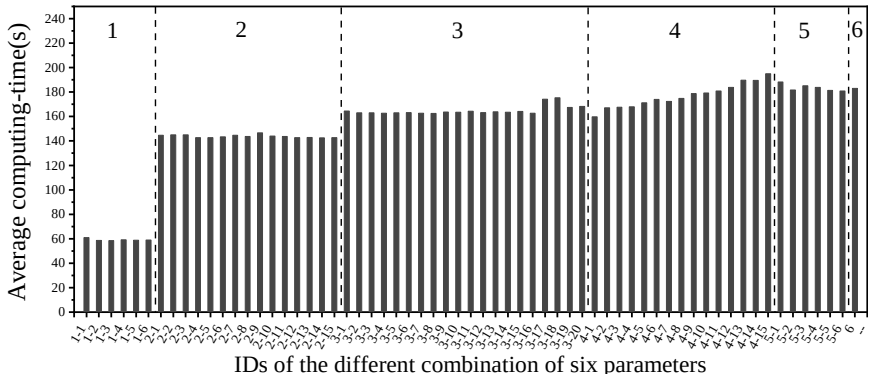

Fig. 12 The average computing-time with the different combinations of six parameters

Table 5 IDs and estimation results of different parameter combinations

Feature numbers	Combination	ID	$\bar{A}_{op}$	$\bar{T}$ (20 nodes)
1	P1	1-1	0.301	60.98
	P2	1-2	0.468	58.63
	P3	1-3	0.395	58.46
	P4	1-4	0.321	59.08
	P5	1-5	0.391	58.74
	P6	1-6	0.284	58.90
2	P1-P2	2-1	0.505	144.61
	P1-P3	2-2	0.487	144.92
	P1-P4	2-3	0.424	144.99
	P1-P5	2-4	0.450	142.74
	P1-P6	2-5	0.436	142.72
	P2-P3	2-6	0.551	143.36
	P2-P4	2-7	0.604	144.66
	P2-P5	2-8	0.594	143.69
	P2-P6	2-9	0.480	146.56
	P3-P4	2-10	0.562	144.00
	P3-P5	2-11	0.557	143.70
	P3-P6	2-12	0.429	142.67
	P4-P5	2-13	0.542	142.89
	P4-P6	2-14	0.395	142.50
	P5-P6	2-15	0.429	142.62

Table 5 Continued

Feature numbers	Combination	ID	$\bar{A}_{op}$	$\bar{T}$ (20 nodes)
3	P1-P2-P3	3-1	0.612	164.53
	P1-P2-P4	3-2	0.638	162.94
	P1-P2-P5	3-3	0.652	163.01
	P1-P2-P6	3-4	0.598	162.65
	P1-P3-P4	3-5	0.623	163.01
	P1-P3-P5	3-6	0.614	163.18
	P1-P3-P6	3-7	0.557	162.62
	P1-P4-P5	3-8	0.589	162.45
	P1-P4-P6	3-9	0.596	163.64
	P1-P5-P6	3-10	0.571	163.42
	P2-P3-P4	3-11	0.731	164.34
	P2-P3-P5	3-12	0.699	163.10
	P2-P3-P6	3-13	0.579	163.83
	P2-P5-P6	3-16	0.641	162.63
	P3-P4-P5	3-17	0.690	174.13
	P3-P4-P6	3-18	0.596	175.30
	P3-P5-P6	3-19	0.576	167.35
	P4-P5-P6	3-20	0.570	168.25
4	P1-P2-P3-P4	4-1	0.753	159.73
	P1-P2-P3-P5	4-2	0.717	167.05
	P1-P2-P3-P6	4-3	0.663	167.58
	P1-P2-P4-P5	4-4	0.748	167.87
	P1-P2-P4-P6	4-5	0.713	171.21
	P1-P2-P5-P6	4-6	0.708	174.04
	P1-P3-P4-P5	4-7	0.709	172.30
	P1-P3-P4-P6	4-8	0.680	174.80
	P1-P3-P5-P6	4-9	0.660	178.72
	P1-P4-P5-P6	4-10	0.692	179.29
	P2-P3-P4-P5	4-11	0.815	180.88
	P2-P3-P4-P6	4-12	0.744	183.86
	P2-P3-P5-P6	4-13	0.717	189.77
	P2-P4-P5-P6	4-14	0.757	189.60
	P3-P4-P5-P6	4-15	0.708	195.00
5	P1-P2-P3-P4-P5	5-1	0.823	188.30
	P1-P2-P3-P4-P6	5-2	0.796	181.75
	P1-P2-P3-P5-P6	5-3	0.753	185.20
	P1-P2-P4-P5-P6	5-4	0.788	183.83
	P1-P3-P4-P5-P6	5-5	0.744	181.33
	P2-P3-P4-P5-P6	5-6	0.821	180.90
6	P1-P2-P3-P4-P5-P6	6	0.843	183.00

using subset of it with different number of hidden layer nodes is shown in Figs. 9 and 10. In Fig. 9, as it can be seen, for all cases, the $\bar{A}$s of the BPNN models increases with the number of hidden layer nodes. The growth curves become flat as the number of nodes increases to a certain value. For features 1 to 6, the certain value of the number of nodes is 30, 20, 20, 15, 10 and 10, respectively. In addition, it can be noticed that for different combinations of the feature parameters, optimal average accuracy ($\bar{A}_{op}$, $\bar{A}_{op}$ is calculated as the average of the $\bar{A}$s corresponding to the

Table 6 The occurrence times of different parameter combinations

ID	P1 (PR)	P2 (HP)	P3 (RP)	P4 (FP)	P5 (HF)	P6 (SE)
6	●	●	●	●	●	●
5-1	●	●	●	●	●	○
5-6	●	●	●	●	●	●
4-11	○	●	●	●	●	○
Subtotal ($\bar{A}$ > 0.800)	3	4	4	4	4	2
5-2	●	●	●	●	○	●
5-4	●	●	○	●	●	●
4-14	○	●	○	●	●	●
4-1	●	●	●	●	○	○
5-3	●	●	●	○	●	●
4-4	●	●	○	●	●	○
4-12	○	●	●	●	○	●
5-5	●	○	●	●	●	●
3-14	○	●	○	●	●	○
3-11	○	●	●	●	○	○
4-2	●	●	●	○	●	○
4-13	○	●	●	○	●	●
4-5	●	●	○	●	○	●
4-7	●	○	●	●	●	○
4-6	●	●	○	○	●	●
4-15	○	○	●	●	●	●
Subtotal ($\bar{A}$ > 0.700)	12	17	14	16	15	12
Total	15	21	18	20	19	14

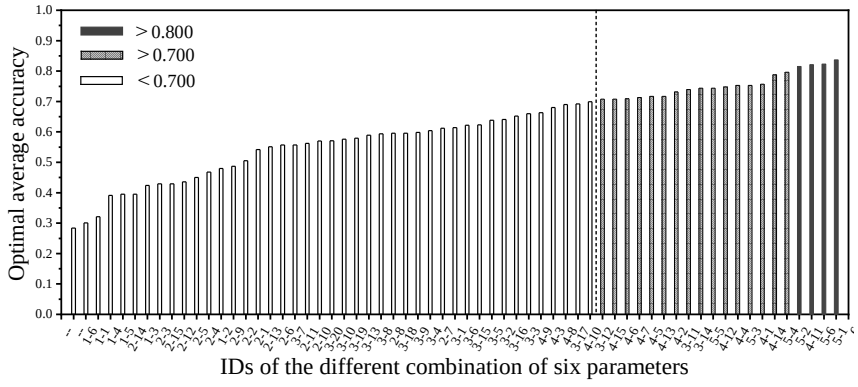

Fig. 13 The order of the optimal average accuracies with the different combinations of six parameters

number of hidden layer nodes after the inflection point) of the neural network model is different as shown in Table 5.

Fig. 10 illustrates variations of the $\bar{T}$ and the $\bar{T}$ per node with the different number of hidden layer nodes and the different combinations of the feature parameters. As shown, for the combinations with the same number of features, the $\bar{T}$s increase linearly and the $\bar{T}$s per node tend to be a fixed value after a sharp drop. This means that when the number of hidden layer nodes is more than the fixed value, the $\bar{T}$ per node value can be calculated by the formula: the $\bar{T}$ = the fixed value × the number of hidden layer nodes, but the performance of the network does not increase. In addition, the rates of increase of the $\bar{T}$s, the $\bar{T}$s and the fixed values of the $\bar{T}$s per node are approximately the same with the combinations at the same number of features. Moreover, further comparison of $\bar{T}$ with different feature combinations as the number of hidden layer nodes = 20 as shown in Fig. 12 and Table 5. As it can be seen, $\bar{T}$ increases with the number of features. The case of 1 feature obtains the minimum value of $\bar{T}$. Additionally, $\bar{T}$ value shows that there is no huge difference for 2 features, 3 features, 4 features, 5 features and 6 features.

Fig. 11 compares $\bar{A}_{op}$ for all combinations of the feature parameters. As it can be seen form this figure, $\bar{A}_{op}$ is different with the same number of features. However, $\bar{A}_{op}$ increases with the number of features. The case of 6

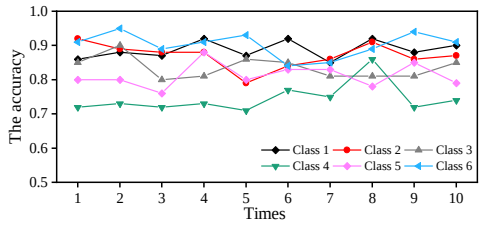

(a) ID=6 (P1-P2-P3-P4-P5-P6) and the number of hidden layer nodes =30

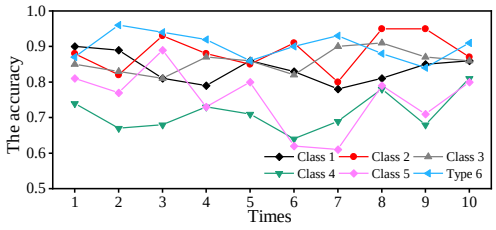

(b) ID=5-1 (P1-P2-P3-P4-P5) and the number of hidden layer nodes =30

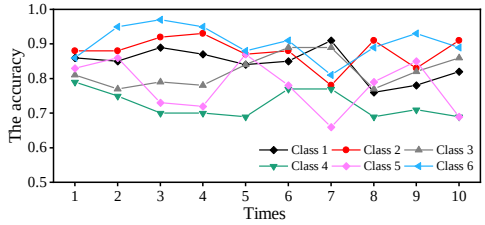

(c) ID=5-6 (P2-P3-P4-P5-P6) and the number of hidden layer nodes =25

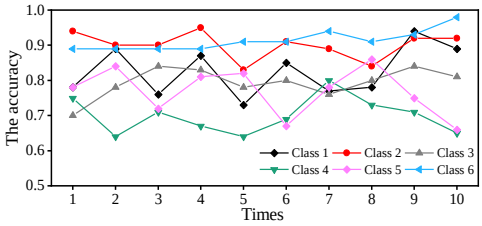

(d) ID=4-11 (P2-P3-P4-P5) and the number of hidden layer nodes =25

Fig. 14 Variations of the accuracy rates of prediction of support pattern selections in 10 experiments with the combination ID 6, ID 5-1, ID 5-6 and ID 4-11

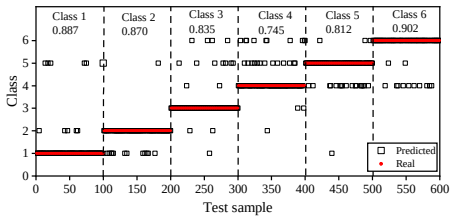

(a) ID=6 (P1-P2-P3-P4-P5-P6) and the number of hidden layer nodes =30

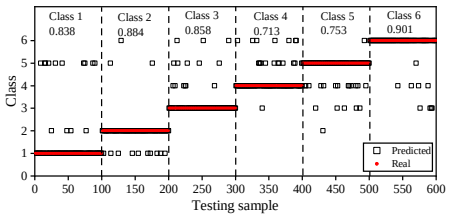

(b) ID=5-1 (P1-P2-P3-P4-P5) and the number of hidden layer nodes =30

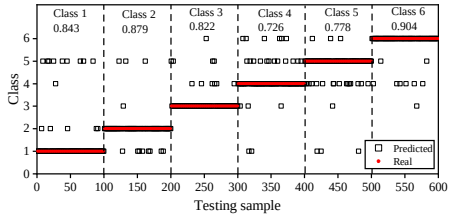

(c) ID=5-6 (P2-P3-P4-P5-P6) and the number of hidden layer nodes =25

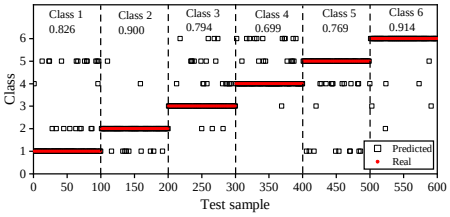

(d) ID=4-11 (P2-P3-P4-P5) and the number of hidden layer nodes =25

Fig. 15 Predicted results of the test sample with the combination ID 6, ID 5-1, ID 5-6 and ID 4-11

Table 7 Statistics of the average accuracy rates and standard deviation of prediction of support pattern selections with the combination ID 6, 5-1, 5-6 and 4-11

ID	Class 1	Class 2	Class 3	Class 4	Class 5	Class 6
6	0.887	0.870	0.835	0.745	0.812	0.902
5-1	0.838	0.884	0.858	0.713	0.753	0.901
5-6	0.843	0.879	0.822	0.726	0.778	0.904
4-11	0.826	0.900	0.794	0.699	0.769	0.914

features obtains the highest results. The case of 1 feature obtains the worst results. This is due to the significant influence of the number of features on the performance of BPNN. Also, it can be observed, the results of the combination ID 6, ID 5-1, ID 5-6 and ID 4-11 of the feature parameters are comparable with each other.

4.3 Sensitivity analysis of each feature parameter

In this subsection, the sensitivity of each feature parameter for estimation performance has been compared. Sensitivity has been measured by counting occurrence times of each parameter in the corresponding combinations of

feature parameters of the experiment cases with superior estimation performance. The sensitivity is defined as the contribution of each parameter to the prediction performance. Fig. 13 shows the excellent combinations of feature parameters with a estimation $\bar{A} > 0.700$, which are ID 6, ID 5-1, ID 5-6 , ID 4-11, ID 5-2, ID 5-4, ID 4-14 , ID 4-1, ID 5-3, ID 4-4, ID 4-12 , ID 5-5, ID 3-14, ID 3-11, ID 4-2 , ID 4-13, ID 4-5, ID 4-7, ID 4-6 and ID 4-15, respectively. Table 6 counts the occurrence times of the feature parameters corresponding to the superior combinations. It must be pointed out that in order to distinguish the sensitivity better, the sum of the occurrence times of the feature parameters when the $\bar{A}$ is greater than 0.7 and 0.8 will be taken as the final score. As it can be observed, the scores of parameters P1, P2, P3, P4, P5 and P6 are 15, 21, 18, 20, 19 and 14, respectively. Thus, the sensitivity of the six parameters is ordered as P2 > P4 > P5 > P3 > P1 > P6 (HP > FP > HF > RP > PR > SE). The SE is a comprehensive parameter measured indirectly, which represents the energy needed to destroy the rock per unit volume. The PR can also be regarded as a comprehensive parameter, which is affected by the mechanical properties of rock and the drilling equipment. HP, FP, HF and RP are directly measured parameters, which are the direct response of drilling equipment to rock performance. The selection of support pattern is mainly determined by the properties of rock. From the sensitivity analysis results of prediction performance, it shows that the sensitivity of the parameters directly measured to the prediction results is higher than the parameters indirectly measured. The HF parameter has the highest sensitivity to the prediction performance of support pattern, while the SE parameter is the lowest.

4.4 Stability of estimation performance

For further comparison of the estimation performance of the BPNN algorithm with different combinations of the feature parameters, stability of the estimation performance with four optimal combinations of feature parameters (combination ID 6, ID 5-1, ID 5-6 and ID 4-11) were analyzed as well. The average of standard deviation (SD) of the *A*s of six class support patterns in 10 experiment cases was counted as index to measure the stability of estimation performance as shown in Table 7. Fig. 14 illustrates variations of the *A*s of estimation results for each class of support patterns in 10 experiments with optimal combinations of feature parameters. In addition, the comparison between the estimated results and the real classes of one of the 10 experiments is shown in Fig. 14. As it can be seen form Table 7, Fig. 14 and Fig. 15, the optimal stability score to 0.066 was obtained by the combination ID 6. The result obtained with the combination ID 4-11 was worst by 0.094. The stability of the estimation performance with four combinations of feature parameters is ordered as ID 6 > ID 5-1 > ID 5-6 > ID 4-11.It can be observed that the order of $\bar{A}$ is the same as the stability.

Through the above analysis, the best predicted results ($\bar{A}$) for six classes of support patterns were 0.887, 0.870, 0.835, 0.745, 0.812 and 0.902, respectively, which were obtained under the combination of six feature parameters (ID=6). These obtained results prove the superiority of the combination with six feature parameters. These selected features can be used further for improving the clustering performance. Although in the literature of the subject, the clusters built by a subset of salient features are more practical and interpretable than clusters built all of the features in most cases, in this study, the clusters built by a subset of salient features has no advantage, which is probably due to the small number of feature parameters. Therefore, for this study, the cluster built by the whole feature parameters has stronger performance, and it can help in better data understanding and interpretation.

5. Conclusions

In this study, an artificial neural network (ANN) model is proposed to estimate the selection of support patterns ahead of tunnel face using measure while drilling (MWD) data including penetration rate (PR), Hammer pressure (HP), rotation pressure (RP), feed pressure (FP), hammer frequency (HF) and specific energy (SE). The proposed ANN model is validated by 318, 649 MWD data obtained from 97 drill holes of a 3.88 km high-speed railway tunnel in Japan. ANN models with different input feature parameters and different hidden layer sizes are constructed for pursuing the best estimation performance. The sensitivity of each feature parameter to the estimation performance of the ANN is compared. The stability of the estimation performance of the ANN models with better performance are analyzed as well. Four different evaluation indices including average accuracy ($\bar{A}$), computing-time ($\bar{T}$), sensitivity and stability are adopted in this study.

- The results show that it is feasible to estimate the selection of support patterns ahead of tunnel face using the ANN by the MWD data. The estimation performance of the ANN is affected by the input layer sizes and hidden layer sizes. The combination of 6 feature parameters outperforms the subset of the entire feature parameters in terms of $\bar{A}$, sensitivity and stability.
- As a reminder, although $\bar{T}$ increases with the number of feature parameters, there is on huge difference for 2 to 6 feature parameters. A hidden layer size greater than 30 neurons has no optimizing effect on the estimation performance.
- The sensitivity of the 6 feature parameters is ordered as HP > FP > HF > RP > PR > SE. The stability of the estimation performance with four better combinations of feature parameters is ordered as ID 6 > ID 5-1 > ID 5-6 > ID 4-11(ID 6: combination of PR, HP, RP,FP, HF and SE; ID 5-1: combination of PR, HP, RP,FP and HF; ID 5-6: combination of HP, RP,FP, HF and SE; ID 4-11: combination of PR, HP, RP and FP). The $\bar{A}$ is the same order as the stability.
- Although it has a slightly larger $\bar{T}$, the ANN model with 6 feature parameters and the 30 hidden layer nodes is proposed as optimal model considering all indices. The

results confirm that the proposed combination with six feature parameters is effective for tunnel support pattern estimation. Estimation of the selection of support patterns ahead of tunnel face in advance using the ANN technology can improve the safety of tunnel excavation and bring considerable benefits in time and cost.

In the present study, the commonly used the error back-propagation neural network (BPNN) algorithm is utilized to demonstrate the correlation between the MWD data and the support patterns. As a preliminary work, the ANN models with other outstanding algorithms are not adopted but will be considered in the future studies. The present study established the BPNN models with all the MWD data parameters, which is therefore merely an initial step to explore the concerned topic. Composition of parameters based on the MWD data need to be considered to improve the estimation performance of the ANN. Besides, more verification and analysis based on other tunnel projects under similar geological conditions should be carried out to understand the adaptability of the proposed ANN estimation model in the future works.

Acknowledgments

The authors gratefully acknowledge support of Civil Engineering Department, Technical Division, Konoike Construction Japan for providing field data and sharing experience on tunnel construction.

References

Basu, J.K., Bhattacharyya, D. and Kim, T. (2010), "Use of artificial neural network in pattern recognition", *Int. J. Software Eng. Appl.*, **4**(2).

Ben Ali, J., Fnaiech, N., Saidi, L., Chebel-Morello, B. and Fnaiech, F. (2015), "Application of empirical mode decomposition and artificial neural network for automatic bearing fault diagnosis based on vibration signals", *Appl. Acoust.*, **89**, 16-27. https://doi.org/10.1016/j.apacoust.2014.08.016.

Bizjak, K.F. and Petkovšek, B. (2004), "Displacement analysis of tunnel support in soft rock around a shallow highway tunnel at Golovec", *Eng. Geol.*, **75**(1), 89-106. https://doi.org/10.1016/j.enggeo.2004.05.003.

Dahlin, T., Bjelm, L. and Svensson, C. (1999), "Use of electrical imaging in site investigations for a railway tunnel through the Hallandsås Horst, Sweden", *Q. J. Eng. Geol. Hydrogeol.*, **32**(2), 163-172. https://doi.org/10.1144/GSL.QJEG.1999.032.P2.06.

Dreyfus, G. (2005), *Neural Networks: Methodology and Applications*, Springer Science & Business Media,

El-Naqa, A. (2001), "Application of RMR and Q geomechanical classification systems along the proposed Mujib Tunnel route, central Jordan", *B. Eng. Geol. Environ.*, **60**(4), 257-269. https://doi.org/10.1007/s100640100112.

Elyasi, A., Javadi, M., Moradi, T., Moharrami, J., Parnian, S. and Amrac, M. (2016), "Numerical modeling of an umbrella arch as a pre-support system in difficult geological conditions: A case study", *B. Eng. Geol. Environ.*, *75*(1), 211-221. https://doi.org/10.1007/s10064-015-0738-5.

Friant, J.E., Bauer, R.A., Gross, D.L., May, M. and Lach, J. (1997), "Pipetron tunnel construction issues", Fermi National Accelerator Lab.(FNAL), Batavia, Illinois, U.S.A.

Galende-Hernández, M., Menéndez, M., Fuente, M.J. and Sainz-Palmero, G.I. (2018), "Monitor-while-drilling-based estimation of rock mass rating with computational intelligence: The case of tunnel excavation front", *Autom. Constr.*, **93**, 325-338. https://doi.org/10.1016/j.autcon.2018.05.019.

García-Pedrajas, N., Hervás-Martínez, C. and Ortiz-Boyer, D. (2005), "Cooperative coevolution of artificial neural network ensembles for pattern classification", *IEEE T. Evol. Comput.*, **9**(3), 271-302. https://doi.org/10.1109/TEVC.2005.844158.

Garson, G.D. (1998), *Neural Networks: An Introductory Guide for Social Scientists*, Sage, London, U.K.

Ghorbani, A., Hasanzadehshooiili, H. and Sadowski, Ł. (2018), "Neural prediction of tunnels' support pressure in elasto-plastic, strain-softening rock mass", *Appl. Sci.*, **8**(5), 841. https://doi.org/10.3390/app8050841.

Ghosh, R., Schunnesson, H. and Kumar, U. (2015), "The use of specific energy in rotary drilling: The effect of operational parameters", *Proceedings of the 37th International Symposium on the Application of Computers and Operations Research in the Mineral Industry*, Fairbanks, Alaska, U.S.A., May.

Gong, Q., Yin, L. and She, Q. (2013), "TBM tunneling in marble rock masses with high in situ stress and large groundwater inflow: A case study in China", *B. Eng. Geol. Environ.*, **72**(2), 163-172. https://doi.org/10.1007/s10064-013-0460-0.

Guan, Z., Jiang, Y. and Tanabashi, Y. (2009), "Rheological parameter estimation for the prediction of long-term deformations in conventional tunnelling", *Tunn. Undergr. Sp. Tech.*, **24**(3), 250-259. https://doi.org/10.1016/j.tust.2008.08.001.

Hecht-Nielsen, R. (1987), "Kolmogorov's mapping neural network existence theorem", *Proceedings of the International Conference on Neural Networks*, Alexandria, Virginia, U.S.A., October.

Hsu, K.L., Gupta, H.V. and Sorooshian, S. (1995), "Artificial neural network modeling of the rainfall-runoff process", *Water Resour. Res.*, **31**(10), 2517-2530. https://doi.org/10.1029/95WR01955.

Humstad, T., Høien, A.H., Kveen, A. and Hoel, J.E. (2012), "Complete software overview of rock mass and support in Norwegian road tunnels", *Proceedings of the ISRM International Symposium - EUROCK 2012*, Stockholm, Sweden, May.

Hush, D.R. (1989), "Classification with neural networks: A performance analysis", *Proceedings of the IEEE International Conference on Systems Engineering*, Fairborn, Ohio, U.S.A., August.

Hussain, S., Mohammad, N., Khan, M., Rehman, Z.U. and Tahir, M. (2016), "Comparative analysis of rock mass rating prediction using different inductive modeling techniques", *Int. J. Min. Eng. Miner. Process.*, **5**(1), 9-15. https://doi.org/10.5923/j.mining.20160501.02.

Kanellopoulos, I. and Wilkinson, G.G. (1997), "Strategies and best practice for neural network image classification", *Int. J. Remote Sens.*, **18**(4), 711-725. https://doi.org/10.1080/014311697218719.

Kaya, A., Bulut, F. and Sayin, A. (2011), "Analysis of support requirements for a tunnel portal in weak rock: A case study from Turkey", *Sci. Res. Essays*, **6**(31), 6566-6583. https://doi.org/10.5897/SRE11.1691.

Kim, C.Y., Bae, G.J., Hong, S.W., Park, C.H., Moon, H.K. and Shin, H.S. (2001), "Neural network based prediction of ground surface settlements due to tunnelling", *Comput. Geotech.*, **28**(6), 517-547. https://doi.org/10.1016/S0266-352X(01)00011-8.

Kontogianni, V., Tzortzis, A. and Stiros, S. (2004), "Deformation and failure of the Tymfristos tunnel, Greece", *J. Geotech. Geoenviron. Eng.*, **130**(10), 1004-1013. https://doi.org/10.1061/(ASCE)1090-0241(2004)130:10(1004).

Koopialipoor, M., Ghaleini, E.N., Tootoonchi, H., Jahed Armaghani, D., Haghighi, M. and Hedayat, A. (2019), "Developing a new intelligent technique to predict overbreak in tunnels using an artificial bee colony-based ANN", *Environ. Earth Sci.*, ***78***(5), 165. https://doi.org/10.1007/s12665-019-8163-x.

Kumar, R., Kumaraswamidhas, L.A., Murthy, V.M.S.R. and Vettivel, S.C. (2019), "Experimental investigations on machine vibration in blast-hole drills and optimization of operating parameters", *Measurement*, **145**, 803-819. https://doi.org/10.1016/j.measurement.2019.05.069.

Kun, M. and Onargan, T. (2013), "Influence of the fault zone in shallow tunneling: A case study of Izmir Metro Tunnel", *Tunn. Undergr. Sp. Tech.*, **33**, 34-45. https://doi.org/10.1016/j.tust.2012.06.016.

Kwon, S. and Lee, C. (2018)," "HM analysis for an in situ experiment using FLAC3D-TOUGH2 and an artificial neural network", *Geomech. Eng.*, **16**(4), 363-373. http://doi.org/10.12989/gae.2018.16.4.363.

Leu, S.S.,Chen, C.N. and Chang, S.L. (2001), "Data mining for tunnel support stability: Neural network approach", *Autom. Constr.*, **10**(4), 429-441. https://doi.org/10.1016/S0926-5805(00)00078-9.

Li, L., Li, S., Zhao, Y., Wang, H., Liu, Q., Yuan, X., Zhao, Y. and Zhang, Q. (2012), "Spatial deformation mechanism and load release evolution law of surrounding rock during construction of super-large section tunnel with soft broken surrounding rock masses", *Chin. J. Rock Mech. Eng.*, **10**, 2109-2118.

Lindén, P. (2005), "Val av borrklass kopplat till MWD, bergklass samt vattenflöde vid projektet Hallandsås".

Liu, J., Sakaguchi, O., Ishizu, S., Luan, H., Han, W. and Jiang, Y. (2020), "Application of specific energy in evaluation of geological conditions ahead of tunnel face", *Energies*, **13**(4), 909. https://doi.org/10.3390/en13040909.

Lo, S.C.B., Chan, H.P., Lin, J.S., Li, H., Freedman, M.T. and Mun, S.K. (1995), "Artificial convolution neural network for medical image pattern recognition", *Neural Networks*, **8**(7-8), 1201-1214. https://doi.org/10.1016/0893-6080(95)00061-5.

Mahdevari, S. and Torabi, S.R. (2012), "Prediction of tunnel convergence using artificial neural networks", *Tunn. Undergr. Sp. Tech.*, **28**, 218-228. https://doi.org/10.1016/j.tust.2011.11.002.

Mahdevari, S., Torabi, S.R. and Monjezi, M. (2012), "Application of artificial intelligence algorithms in predicting tunnel convergence to avoid TBM jamming phenomenon", *Int. J. Rock Mech. Min. Sci.*, **55**, 33-44. https://doi.org/10.1016/j.ijrmms.2012.06.005.

McCulloch, W.S. and Pitts, W. (1943), "A logical calculus of the ideas immanent in nervous activity", *B. Math. Biophys.*, **5**(4), 115-133. https://doi.org/10.1007/BF02478259.

Mikaeil, R., Haghshenas, S.S., Shirvand, Y., Hasanluy, M.V. and Roshanaei, V. (2016), "Risk assessment of geological hazards in a tunneling project using harmony search algorithm (case study: Ardabil-Mianeh railway tunnel)", *Civ. Eng. J.*, **2**(10), 546-554. https://doi.org/10.28991/cej-2016-00000057.

Miura, K. (2003), "Design and construction of mountain tunnels in Japan", *Tunn. Undergr. Sp. Tech.*, **18**(2), 115-126. https://doi.org/10.1016/S0886-7798(03)00038-5.

Navarro, J., Sanchidrian, J.A., Segarra, P., Castedo, R., Paredes, C. and Lopez, L.M. (2018), "On the mutual relations of drill monitoring variables and the drill control system in tunneling operations", *Tunn. Undergr. Sp. Tech.*, **72**, 294-304. https://doi.org/10.1016/j.tust.2017.10.011.

Nikafshan Rad, H., Jalali, Z. and Jalalifar, H. (2015), "Prediction of rock mass rating system based on continuous functions using Chaos–ANFIS model", *Int. J. Rock Mech. Min. Sci.*, **73**, 1-9. https://doi.org/10.1016/j.ijrmms.2014.10.004.

Nilsen, B. (2015), "Main challenges for deep subsea tunnels based on norwegian experience", *J. Kor. Tunn. Undergr. Sp. Assoc.*, **17**(5), 563-573. https://doi.org/10.9711/KTAJ.2015.17.5.563.

Ocak, I. and Seker, S.E. (2013), "Calculation of surface settlements caused by EPBM tunneling using artificial neural network, SVM, and Gaussian processes", *Environ. Earth Sci.*, **70**(3), 1263-1276. https://doi.org/10.1007/s12665-012-2214-x.

Paola, J. (1994), "Neural network classification of multispectral imagery", M.Sc. Thesis, The University of Arizona, Tucson, Arizona, U.S.A.

Park, J., Lee, K.H., Kim, B.K., Choi, H. and Lee, I.M. (2017), |Predicting anomalous zone ahead of tunnel face utilizing electrical resistivity: II. Field tests", , *Tunn. Undergr. Sp. Tech.*, **68**, 1-10. https://doi.org/10.1016/j.tust.2017.05.017.

Qiu, D., Li, S., Xu, Y., Tian, H. and Yan, M. (2014), "Advanced prediction of surrounding rock classification based on digital drilling technology and QGA-RBF neural network", *Rock Soil Mech.*, (7), 2013-2018.

Rafiq, M.Y., Bugmann, G. and Easterbrook, D.J. (2001), "Neural network design for engineering applications", *Comput. Struct.*, **79**(17), 1541-1552. https://doi.org/10.1016/S0045-7949(01)00039-6.

Ripley, B.D. (1993), "Statistical aspects of neural networks", *Networks Chaos Stat. Probab. Aspects*, **50**, 40-123.

Schunnesson, H. (1997), "Drill process monitoring in percussive drilling for location of structural features, lithological boundaries and rock properties, and for drill productivity evaluation", Ph.D. Dissertation, Luleå University of Technology, Luleå, Sweden.

Schunnesson, H. (1998), "Rock characterisation using percussive drilling", *Int. J. Rock Mech. Min. Sci.*, **35**(6), 711-725. https://doi.org/10.1016/S0148-9062(97)00332-X.

Schunnesson, H. (1996), "RQD predictions based on drill performance parameters", *Tunn. Undergr. Sp. Tech.*, **11**(3), 345-351. https://doi.org/10.1016/0886-7798(96)00024-7.

Schunnesson, H., Elsrud, R. and Rai, P. (2011), "Drill monitoring for ground characterization in tunnelling operations", *Proceedings of the International Symposium on Mine Planning and Equipment Selection*, Almaty, Kazakhstan, October.

Segui, J. and Higgins, M. (2002), "Blast design using measurement while drilling parameters", *Fragblast*, **6**(3-4), 287-299. https://doi.org/10.1076/frag.6.3.287.14052.

Singh, B., Jethwa, J., Dube, A. and Singh, B. (1992), "Correlation between observed support pressure and rock mass quality", *Tunn. Undergr. Sp. Tech.*, **7**(1), 59-74. https://doi.org/10.1016/0886-7798(92)90114-W.

Soupios, P., Loupasakis, C. and Vallianatos, F. (2008), "Reconstructing former urban environments by combining geophysical electrical methods and geotechnical investigations—an example from Chania, Greece", *J. Geophys. Eng.*, ***5***(2), 186-194. https://doi.org/10.1088/1742-2132/5/2/005.

Suwansawat, S. and Einstein, H.H. (2006), "Artificial neural networks for predicting the maximum surface settlement caused by EPB shield tunneling", *Tunn. Undergr. Sp. Tech.*, **21**(2), 133-150. https://doi.org/10.1016/j.tust.2005.06.007.

Toghroli, A., Mohammadhassani, M., Suhatril, M., Shariati, M. and Ibrahim, Z. (2014), "Prediction of shear capacity of channel shear connectors using the ANFIS model", *Steel Compos. Struct.*, **17**(5), 623-639. http://dx.doi.org/10.12989/scs.2014.17.5.000.

Utt, W.K. (1999), "Neural network technology for strata strength characterization", *Proceedings of the International Joint Conference on Neural Networks*, Middleton, Wisconsin, U.S.A., July.

Utt, W.K., Miller, G.G., Howie, W.L. and Woodward, C.C. (2002), "Drill monitor with strata strength classification in near-real time", Report of Investigations, No. 2002-2141, National

Institute for Occupational Safety and Health 9658.
van Eldert, J., Schunnesson, H. and Johansson, D. (2017), "The history and future of rock mass characterisation by drilling in drifting: From sledgehammer to PC-tablet", *Proceedings of the 26th International Symposium on Mine Planning and Equipment Selection*, Luleå, Sweden, August.
van Eldert, J., Schunnesson, H.,Johansson, D. and Saiang, D. (2019), "Application of measurement while drilling technology to predict rock mass quality and rock support for tunnelling", *Rock Mech*. *Rock Eng*., 1-10. https://doi.org/10.1007/s00603-019-01979-2.
Wang, X. and Meng, F. (2018), "Statistical analysis of large accidents in China's coal mines in 2016", *Nat*. *Hazards*, **92**(1), 311-325. https://doi.org/10.1007/s11069-018-3211-5.
Xue, X. (2019), "Application of a support vector machine for prediction of piping and internal stability of soils", *Geomech*. *Eng*., **18**(5), 493-502. http://doi.org/10.12989/gae.2019.18.5.493.
Yang, Y. and Zhang, Q. (1997), "A hierarchical analysis for rock engineering using artificial neural networks", *Rock Mech*. *Rock Eng*., **30**(4), 207-222. https://doi.org/10.1007/BF01045717.
Yi, X., Chen, W., Li, S. and Dai, Y. (2006), "Application of bp neural network to back analysis of forked tunnel displacement", *Chin*. *J*. *Rock Mech*. *Eng*., **25**(s2), 3927-3932.
Zhang, S., Li, Y. and Xu, C. (2017), "Application of black box model for height prediction of the fractured zone in coal mining", *Geomech*. *Eng*., **13**(6), 997-1010. http://doi.org/10.12989/gae.2017.13.6.997.
Zhou, F., Sun, W., Shao, J., Kong, L. and Geng, X. (2020), "Experimental study on nano silica modified cement base grouting reinforcement materials", *Geomech*. *Eng*., **20**(1), 67-73. https://doi.org/10.12989/gae.2020.20.1.067.